Nanopore formation on unilamellar vesicles of long- and short-chain lipids

Norifumi L. Yamada,[1,*] Mafumi Hishida,[2] and Naoya Torikai[1]
[1]*Neutron Science Laboratory, High Energy Accelerator Research Organization, Tsukuba 305-0801, Japan*
[2]*Department of Physics, Kyoto University, Kyoto 606-8502, Japan*
(Received 7 October 2008; published 13 March 2009)

The structure of unilamellar vesicles (ULVs), comprising long- and short-chain lipids, was investigated, and the formation of nanopores on the surface of the ULVs was confirmed under the condition of long- and short-chain lipids being separated. It was also revealed that the behavior of the structural phase transition from ULVs to bilayered micelles (bicelles) depends on the number of nanopores formed on the surface of the ULVs. Because both the rim structures of nanopores and bicelles are considered to be microdomains of short-chain lipids, this phase behavior was explained by considering the kinetic pathway of the growth of the rim domain. It was concluded that the phase segregation of lipids plays an essential role in the rim formation of nanopores as well as bicelles.

DOI: 10.1103/PhysRevE.79.032902 PACS number(s): 87.14.Cc, 61.05.fg, 87.16.D−

Cells and their organelles are enclosed by biomembranes comprising lipid bilayers. Lipid molecules self-assemble bilayers in water due to their amphiphilic property; thus far, bilayers comprising synthetic lipids have been investigated to clarify the physical properties of biomembranes. In particular, unilamellar vesicles (ULVs) are often used as model cells because they mimic the spaces enclosed by a lipid bilayer.

In a real cell, one of the methods that enable the exchange in materials through a biomembrane is the creation of pores on the cell surface. For example, channel proteins create nanopores on biomembranes and regulate the flow of ions by opening and closing the pores. Therefore, many attempts have been made to create similar pores on lipid bilayers by adding proteins [1], peptides [2], etc., and the created pores have been used as a model system to understand the material transportation process in living cells [3]. However, few researches have been conducted on the mechanism of the formation of nanopores from the viewpoint of physics.

To simplify this matter, we focused on the nanopores formed on the surface of simple membranes without any large biomolecules, that is, perforated membranes comprising a mixture of long- and short-chain lipids. According to previous experimental results of neutron scattering [4–6], light scattering [7], and electron microscopy [8] on dimyristoylphosphatidylcholine (DMPC) (14 carbons/chain) and dihexanoylphosphatidylcholine (DHPC) (6 carbons/chain) mixtures, a phase transition occurs with a drastic structural change at the chain melting temperature of DMPC, T_c (~24 °C), as shown in Fig. 1. Below T_c, bilayered micelles (bicelles; approximately one hundred angstroms in radius) appear because DHPC molecules are stable in forming the rim of a DMPC bilayer due to a mismatch in the chain lengths. Above T_c, the bicelles fuse to form various structures such as vesicles, lamellae, etc., depending on the whole lipid concentration, ϕ_l, even when the molar ratio of DHPC to DMPC is fixed. It has been reported that nanopores (tens of angstroms in radius) were observed in the lamellar phase, in which the rim was stabilized by the DHPC molecules as in the case of bicelles [4]. This perforated membrane suitably mimics a biomembrane with pores as a lipid bilayer with biomolecules.

When ϕ_l is less than 2–3 vol % [4,5], ULVs (several hundreds of angstroms in radius) may be created instead of perforated lamellae. Although the structural transition accompanying bicelle fusion is basically reversible, temperature hysteresis was reported below approximately 1 vol % [6]; large bicelles (several hundreds of angstroms in radius) or ULVs are formed when the temperature crosses T_c from the above. Here, we emphasize that perforated ULVs can be created easily if nanopores are formed as in the case of lamellae. These perforated ULVs can potentially be used as a model system in exploring the function of nanopores in the intermembrane material transportation process.

Recently, it was shown by fluorescence measurement that ULVs comprising DMPC, DHPC, and small amount of charged lipids are basically impermeable, that is, nanopores were not formed on the surface of ULVs [9]. However, it was not clarified why the nanopores disappeared, unlike the case of lamellae [4]. In this study, the formation of nanopores on the surface of ULVs comprising DMPC and DHPC was con-

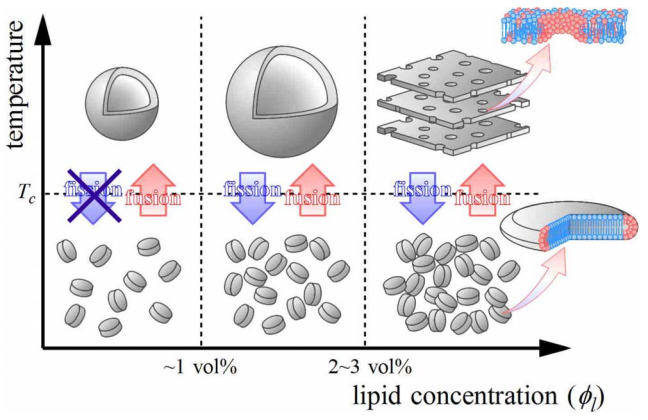

FIG. 1. (Color online) Schematic illustration of phase transition in a mixture of long- and short-chain lipids at different temperatures and lipid concentrations, ϕ_l.

*yamadan@post.kek.jp

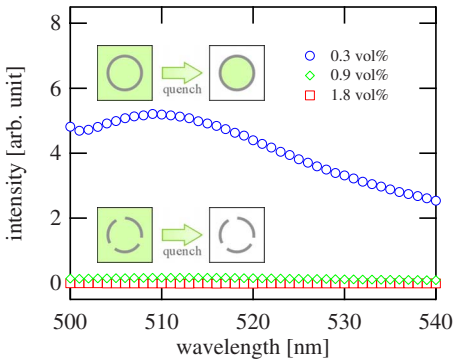

FIG. 2. (Color online) Fluorescence spectra of calcein 5 min after adding $CoCl_2$ at 50 °C. Since Co^{2+} ions penetrated the ULVs through nanopores and quenched the calceins completely, no fluorescence was observed at 1.8 and 0.9 vol %.

firmed by fluorescence measurement and small-angle neutron scattering (SANS). In addition, the relationship between the formation of nanopores on the surface of ULVs and temperature hysteresis on the transition from ULVs to bicelles was found.

DMPC and DHPC were purchased from Avanti Polar Lipids Inc.; D_2O, from Isotec; and $CaCl_2$, from Kishida Chemical Inc. The materials were used without further purification. The sample was prepared as follows. First, a lipid mixture having the molar ratio [DMPC]:[DHPC]=4.6:1 was dissolved in an organic solvent (volume ratio of methanol:chloroform=1:2). After the evaporation of the organic solvent, the obtained lipid mixture was hydrated with a D_2O solution of 3 mM $CaCl_2$ to ϕ_l=2.4 vol % at room temperature. Next, the sample temperature was cycled (5–50 °C) more than five times to obtain a homogeneous solution. Furthermore, the homogeneous lipid solution was diluted to 0.30–2.1 vol % while maintaining the temperature below T_c to suppress the phase transition of the sample. In this condition, ULVs were spontaneously formed above T_c [5].

Fluorescence measurements were performed using a Hitachi F-7000 fluorescence spectrophotometer. In this experiment, 1 mL of the sample including 1 μM calcein {bis[N,N-bis(carboxymethyl)aminomethyl]fluorescein; excitation wavelength: 488 nm, emission wavelength: 515 nm} was heated from 0 to 50 °C to create ULVs, and it was then mixed with 1 μL of 20 mM $CoCl_2$ solution at 50 °C. Since Co^{2+} ions, which quench calcein, cannot permeate lipid bilayers, the fluorescence intensity can be sustained for over an hour as long as nanopores do not form on the surface of the ULVs [10]. On the other hand, the fluorescence intensity will be immediately quenched if nanopores form on the surface of the ULVs. Hence, the fluorescent spectra were observed 5 min after adding $CoCl_2$ to examine the perforation of ULVs.

Figure 2 shows typical fluorescent spectra for different ϕ_l at 50 °C. The fluorescent spectra clearly indicated that the fluorescence of calcein disappeared for ϕ_l=0.90 and 1.8 vol % while it was sustained for ϕ_l=0.30 vol %. This indicated that nanopores were formed on the surface of ULVs except for ϕ_l=0.30 vol %.

The SANS experiments were performed using SANS-U at the C1-2 port of JRR-3 at the Japan Atomic Energy Agency (JAEA), Tokai [11]. An incident neutron beam with a wavelength of 7 Å ($\Delta\lambda/\lambda$=10%) was obtained by using a velocity selector; the distances between the sample and the detector were 1.5 and 12 m. To investigate the structural difference between before and after increasing of the temperature, the SANS experiments were performed at 20 °C (below T_c), 50 °C (above T_c), and again at 20 °C. Seven samples with ϕ_l=0.30–2.1 vol % were stored at 0 °C in ice water and set in a sample holder at 20 or 50 °C immediately before performing the experiment. Since the obtained two-dimensional data were isotropic, they were azimuthally averaged to provide one-dimensional data.

The obtained SANS profiles were analyzed by full fitting to quantitatively discuss the mechanism of the formation of nanopores and temperature hysteresis. The scattering intensity $I(q)$ is described as

$$I(q) = n\langle |f(q)|^2 s(q)\rangle + I_{\text{inc}}, \tag{1}$$

where n is the number density of particles; $f(q)$ is the form factor of a particle; $s(q)$ is the structure factor describing the interference between particles; I_{inc} is the incoherent scattering, which is independent of the scattering angle; and $\langle\cdots\rangle$ is the ensemble average of the size distribution. The form factors of bicelles and ULVs were assumed to be those of disks and hollow spheres [12], respectively, which include structural parameters such as the disk radius R_D, vesicle inner radius R_V, disk thickness δ_D, and vesicle thickness δ_V. While fitting the data, δ_D and δ_V were fixed at 44.3 and 36.9 Å, respectively, which were estimated from the temperature dependence of the head area and volume of a DMPC molecule [13]. The structure factor of the bicelles and ULVs was assumed to be the same as that of hard spheres [14], and their size distribution was modeled using the Schultz distribution [12].

Figure 3 shows typical SANS profiles for different ϕ_l and temperatures (solid lines denote the results of fitting). At 20 °C, before heating to 50 °C, typical bicelle profiles appeared while characteristic fringes of ULVs were observed at 50 °C. On the other hand, various structures due to temperature hysteresis depending on ϕ_l were observed at 20 °C after cooling from 50 °C, which was consistent with the result of the previous SANS experiments [6]. For $1.5 \leq \phi_l \leq 2.1$ vol %, the bicelle profiles were recovered at 20 °C after cooling from 50 °C. On the other hand, the bicelles observed at 20 °C after cooling from 50 °C were larger than the initial ones observed before heating to 50 °C for $0.6 \leq \phi_l \leq 1.2$ vol % because a shoulder corresponding to twice the bicelle diameter shifted toward a lower q. Moreover, the fringes due to the ULVs were sustained for ϕ_l=0.30 vol %; the ULVs coexisted with the large bicelles. These structures did not recover their initial configurations for over a month.

Figure 4 indicates the ϕ_l dependence of R_D and R_V evaluated from the fitting (all the statistical errors of R_D and R_V are less than 1%, and the typical polydispersity index is within 0.20 ± 0.02). R_D of the initial bicelles decreased with increasing ϕ_l at 20 °C before heating to 50 °C while that of the large bicelles increased with ϕ_l at 20 °C after cooling to 50 °C; R_V also increased with ϕ_l at 50 °C (although Ref. [5]

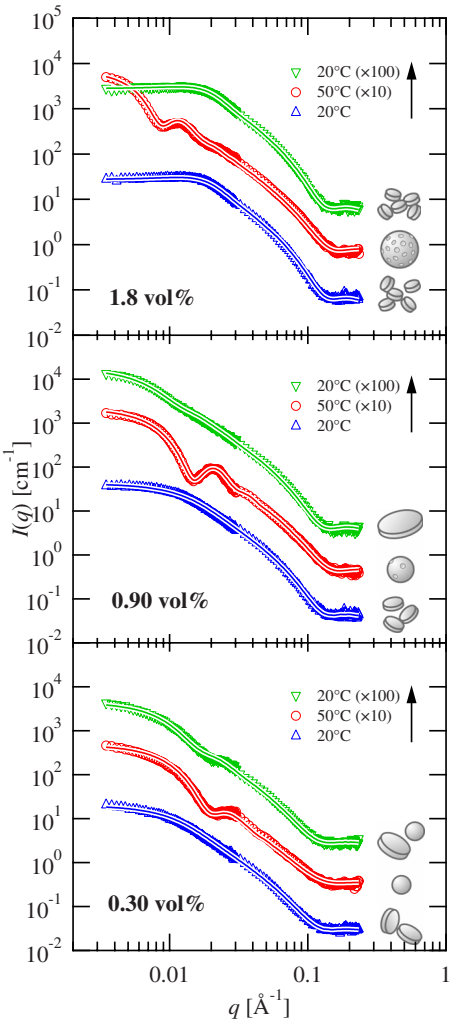

FIG. 3. (Color online) Typical SANS profiles for different temperatures and ϕ_l (arrows indicate temperature sequence). At 20 °C, after cooling from 50 °C, small bicelles, large bicelles, and ULVs appeared at 1.8, 0.90, and 0.30 vol %, respectively. Some profiles have been shifted for better visualization.

claims that R_V is independent of ϕ_l, this ϕ_l dependence of R_V was well reproduced). If the DMPC and DHPC molecules are completely separated from each other, the amount of DHPC in the molar ratio, θ, can be expressed as

$$\theta = \frac{[\mathrm{DHPC}]}{[\mathrm{DMPC}]} \propto \frac{A_{\mathrm{rim}}}{A_{\mathrm{plane}}} \simeq \frac{\delta_D}{R_D}, \tag{2}$$

where A_{rim} and A_{plane} denote the area of a rim and planes of bicelles, respectively. This indicates that R_D should be constant for a fixed θ even if ϕ_l varies, which appears to be inconsistent with the experimental results.

The reason for the ϕ_l dependence of the R_D of the initial bicelles has already been revealed by previous experiments [7,8]. According to these studies, DHPC molecules are detached from membranes on dilution because they are slightly soluble in water (the critical micelle concentration of DHPC is approximately 15 mM while that of DMPC is very low). This implies that the effective θ increases with ϕ_l. Being

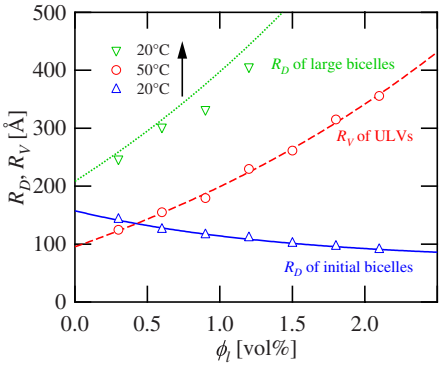

FIG. 4. (Color online) ϕ_l dependence of R_D at 20 °C and R_V at 50 °C (an arrow indicates a temperature sequence). Solid and dashed lines indicate the result of fitting to an empirical function at 20 (before heating) and 50 °C, respectively. The dotted line for large bicelles at 20 °C (after heating) observed below 1.2 vol % was reconstructed from the dashed line by using Eq. (3).

inversely proportional to θ, as given by Eq. (2), R_D of initial bicelles decreases with increasing ϕ_l. This ϕ_l dependence of the effective θ can also explain that of R_V considering the energy balance between the bending energy of a ULV surface and the line tension of a bicelle rim because the increase in the effective θ resulted in a decrease in the line tension (see Refs. [6,12], and references therein for details).

We emphasize here that a decrease in the effective θ results in the disappearance of nanopores on the surface of ULVs; for example, no nanopores were present for ϕ_l =0.30 vol %. Since the rims of nanopores were considered as microdomains of DHPC molecules, the formation of nanopores can be elucidated by the phase segregation between lipid species, as in the case of a mixture of sphingomyelin, unsaturated lipid, and cholesterol [15]. In this sense, temperature may affect the formation of nanopores due to the change in the mixing entropy of lipids, as well as the effective θ. To check the effect of temperature on the fluorescence and SANS experiments, the temperature was decreased from 50 to 30 °C for ϕ_l=0.30 vol %. While the sustained fluorescence intensity at 50 °C gradually decreased for over 20 min after cooling to 30 °C, the ULVs retained their shape and size for at least two days. Although DMPC bilayers become permeable to ions when temperature approaches T_c, they are almost impermeable at 30 °C [16]. Hence, it was concluded that the leakage of ions with decreasing temperature was attributed to the formation of nanopores enhanced by the phase segregation of lipids.

Next, we focused on the formation of large bicelles after increasing the temperature. Since R_D of the large bicelles increased with ϕ_l, similar to R_V, it was anticipated that the large bicelles were transformed from the ULVs. To confirm this speculation, R_D of the large bicelles was evaluated from R_V under the assumption that the volume of a membrane is conserved as follows:

$$R_D = \sqrt{\frac{4\{(R_V + \delta_V)^3 - R_V^3\}}{3\delta_D}}. \tag{3}$$

The dashed line in Fig. 4 is the result of fitting to an empirical function, $R_V = Ae^{a\phi_l} + B$, and the dotted line denotes the

R_D reconstructed from the dashed line using Eq. (3). Since this line followed R_D of the large bicelles well, it was concluded that the large bicelles were transformed from the ULVs. The slight difference between the experimental values and the calculated curve around $\phi_l = 1$ vol % may be due to nanopores on ULVs.

To understand the mechanism of the temperature hysteresis, we focused on the rim domain growth of bicelles beginning at nanopores on the surface of ULVs. For $\phi_l = 0.30$ vol %, there was no nanopore which is the nucleus for the formation of a rim domain of a bicelle, that is, nanopores. Therefore, the ULVs were stable even below T_c. With increasing ϕ_l, i.e., effective θ, the formation of nanopores was enhanced. Since the number of nanopores was, however, small for $0.6 \leq \phi_l \leq 1.2$ vol %, a single rim domain grew in the transition, and large bicelles were sequentially formed. With further increase in ϕ_l, many rim domains grew and small bicelles the same as those before heating to 50 °C were formed. Hence, it was concluded that the kinetic pathway of the rim domain growth results in the temperature hysteresis, which is governed by the number of nanopores formed on the surface of ULVs.

In summary, the formation of nanopores on the surface of ULVs comprising long- and short-chain lipids was confirmed. Furthermore, various types of structures were observed after cooling the ULVs below T_c, that is, ULVs with several nanopores fissured into small bicelles, those with a few nanopores transformed into large bicelles, and those without any nanopores remained stable. These phenomena were understood by means of the formation of rim structures due to the phase segregation between lipid species. This viewpoint could help us clarify the mechanism of nanopore formation in real biomembranes.

The authors acknowledge H. Seto for a critical reading of the manuscript, and S. Okabe, H. Endo, and M. Shibayama for providing technical support in performing the experiments using SANS-U owned by the Institute for Solid State Physics, the University of Tokyo (Proposal Nos. 6563, 7635, and 7853 K). This study was financially supported by the Sasakawa Scientific Research Grant from the Japan Science Society, and a Grant-in-Aid for Young Scientists (Contract No. 20740246) and Creative Scientific Research (Contract No. 16GS0417) from the Ministry of Education, Culture, Sports, Science, and Technology of Japan.

[1] R. J. C. Gilbert, Cell. Mol. Life Sci. **59**, 832 (2002).
[2] B. Bechinger, J. Membr. Biol. **156**, 197 (1997).
[3] L. Brun, M. Pastoriza-Gallego, G. Oukhaled, J. Mathe, L. Bacri, L. Auvray, and J. Pelta, Phys. Rev. Lett. **100**, 158302 (2008).
[4] M. P. Nieh, C. J. Glinka, and S. Krueger, Langmuir **17**, 2629 (2001).
[5] M. P. Nieh, T. A. Harroun, V. A. Raghunathan, C. J. Glinka, and J. Katsaras, Phys. Rev. Lett. **91**, 158105 (2003).
[6] M. P. Nieh, V. A. Raghunathan, S. R. Kline, T. A. Harroun, C. Y. Huang, J. Pencer, and J. Katsaras, Langmuir **21**, 6656 (2005).
[7] K. J. Glover, J. A. Whiles, G. Wu, N. J. Yu, R. Deems, J. O. Struppe, R. E. Stark, E. A. Komives, and R. R. Vold, Biophys. J. **81**, 2163 (2001).
[8] L. van Dam, G. Karlsson, and K. Edwards, Biochim. Biophys. Acta **1664**, 241 (2004).
[9] M.-P. Nieh, J. Katsaras, and X. Qi, Biochim. Biophys. Acta **1778**, 1467 (2008).
[10] D. A. Kendall and R. C. MacDonald, J. Biol. Chem. **257**, 13892 (1982); Anal. Biochem. **134**, 26 (1983).
[11] S. Okabe, M. Nagao, T. Karino, S. Watanabe, T. Adachi, H. Shimizu, and M. Shibayama, J. Appl. Crystallogr. **38**, 1035 (2005).
[12] T. M. Weiss, T. Narayanan, C. Wolf, M. Gradzielski, P. Panine, S. Finet, and W. I. Helsby, Phys. Rev. Lett. **94**, 038303 (2005).
[13] S. Tristram-Nagle, Y. Liu, J. Legleiter, and J. Nagle, Biophys. J. **83**, 3324 (2002); H. I. Petrache, S. Tristram-Nagle, and J. F. Nagle, Chem. Phys. Lipids **95**, 83 (1998); J. F. Nagle and D. A. Wilkinson, Biophys. J. **23**, 159 (1978).
[14] N. W. Ashcroft and J. Lekner, Phys. Rev. **145**, 83 (1966).
[15] T. Baumgart, S. T. Hess, and W. W. Webb, Nature (London) **425**, 821 (2003).
[16] M. C. Blok, E. C. M. van der Neut-Kok, L. L. M. van Deenen, and J. de Gier, Biochim. Biophys. Acta **406**, 187 (1975).